Available online at www.sciencedirect.com
ScienceDirect
Earth and Planetary Science Letters 249 (2006) 188–199
EPSL
www.elsevier.com/locate/epsl

Partial melting experiments of bimineralic eclogite and the role of recycled mafic oceanic crust in the genesis of ocean island basalts

Tetsu Kogiso [a,b,*], Marc M. Hirschmann [c]

[a] *Institute for Research on Earth Evolution (IFREE), Japan Agency for Marine-Earth Science and Technology (JAMSTEC), Yokosuka 237-0061, Japan*
[b] *Department of Earth and Planetary Sciences, Tokyo Institute of Technology, Meguro, Tokyo 152-8551, Japan*
[c] *Department of Geology and Geophysics, University of Minnesota, Minneapolis, MN 55455, USA*

Received 18 January 2006; received in revised form 11 July 2006; accepted 12 July 2006
Available online 17 August 2006
Editor: R.W. Carlson

Abstract

Bimineralic eclogite, which consists solely of garnet and clinopyroxene, is a likely component of some of the ancient recycled crust residing in basalt source regions. It may originate during subduction of altered mid-ocean ridge basalt (MORB) crust, owing to extraction of small degree partial melts or siliceous hydrous fluids. It may also originate by fractional removal of early-formed partial melts from recycled crust or from pyroxenite originating by other processes. We have performed high-pressure experiments on a bimineralic eclogite (B-ECL1) and its mixture with olivine (B-ECL1-OL) at 3 and 5 GPa. Degrees of melting are slightly higher for B-ECL1-OL than for B-ECL1 at given temperatures, suggesting that addition of small amounts of olivine enhances melt productivity of bimineralic eclogite. Solidus and liquidus temperatures of B-ECL1 are slightly higher than those of B-ECL1-OL and MORB-like pyroxenite, but are lower than those of high-MgO pyroxenite and peridotite, suggesting that bimineralic eclogite is not necessarily refractory compared to other likely mantle lithologies. Partial melts of B-ECL1 and B-ECL1-OL are nepheline-normative. Because garnet and clinopyroxene in these compositions partially melt at a eutectic-like minimum with a composition that is nepheline-normative, a wide range of bimineralic eclogite compositions, including that of subducted-crust origin, that consist of garnet and clinopyroxene with compositions similar to those of B-ECL1 can produce nepheline-normative (=alkali −basaltic) liquids. Thus, in contrast to the common assumption that partial melting of recycled oceanic crust produces silicic magmas, we conclude that such lithologies can produce nepheline-normative partial melts if they first experience fractional removal of fluids or melts. The partial melts from B-ECL1 are too low in MgO to be parental to many alkalic OIB, but have low Al_2O_3 and high FeO comparable to those of alkalic OIB, suggesting that bimineralic recycled crust is a potential source for a low-Al_2O_3 and high-FeO component that is necessary for the genesis of alkalic OIB.

Keywords: experimental petrology; partial melting; ocean island basalt; pyroxenite; eclogite

1. Introduction

Mafic lithologies in the mantle, including eclogites and pyroxenites, may have a wide spectrum of origins and compositions [1] and their partial melting behavior is highly varied [2]. At similar pressures, nominally

* Corresponding author. Department of Earth and Planetary Sciences, Tokyo Institute of Technology, Meguro, Tokyo 152-8551, Japan. Tel.: +81 3 5734 2338; fax: +81 3 5734 3538.
E-mail addresses: kogisot@jamstec.go.jp (T. Kogiso), Marc.M.Hirschmann-1@umn.edu (M.M. Hirschmann).

0012-821X/$ - see front matter © 2006 Elsevier B.V. All rights reserved.
doi:10.1016/j.epsl.2006.07.016

volatile-free pyroxenites of different bulk composition can produce partial melts ranging from silicic andesites to highly undersaturated basanites [3–6]. There has been a recent spate of studies documenting the partial melting behavior of a range of eclogite and pyroxenite bulk compositions (e.g., [3–8]), in part focused on their possible role in the genesis of ocean island basalts (OIB) [4,5]. However, an important variety of pyroxenite, bimineralic eclogite, which consists solely of garnet and clinopyroxene, has not been the subject of detailed experimental investigation.

Bimineralic eclogite may be a key variety of mantle heterogeneity and may originate from several different processes in distinct geodynamic environments. One important possibility is that oceanic crust may become bimineralic by removal of free silica during subduction. In addition to garnet and pyroxene, subducted dehydrated oceanic crust contains quartz or its high-pressure polymorphs (±rutile). However, extraction of SiO_2 by a combination of dehydration [9], partial melting [10], and/or evolution of a siliceous supercritical fluid [11] may leave a bimineralic residue. Also, subducted oceanic crust may be hybridized by surrounding peridotite, either through mechanical [12] or diffusive [13] exchange during ~2 Gyr residence in the mantle. These processes are likely to produce a bimineralic lithology or an olivine-bearing pyroxenite, depending on the extent of hybridization.

Bimineralic eclogite may also evolve from more mineralogically complex pyroxenites by the early stages of removal of partial melts in basalt source regions. In addition to garnet and clinopyroxene, many pyroxenites contain variable proportions of other phases, such as olivine, orthopyroxene, Fe–Ti or aluminous oxides, quartz, or kyanite. Experimental evidence suggests that these phases typically are exhausted after a modest fraction (0–15%) of melting [3–6]. If melt is removed from the matrix, a bimineralic residue may result. Note however, that removal of melt from pyroxenite bodies may not be as efficient as for partial melting of a homogeneous mantle, as the rate of compaction is related to the size of the domain [13].

Bimineralic eclogite originating from subducted oceanic crust may play an important role in basalt source regions. The siliceous partial melts of MORB-like pyroxenites [3,6] are unlike the alkalic OIB that typically carry strong signatures of crustal recycling [14,15]. For this reason, some have argued that recycled oceanic crust cannot be the proximal source of such basalts (e.g., [16]). However, if recycled oceanic crust loses its siliceous phases during subduction, residence in the deep mantle, and/or partial melting and interaction with surrounding peridotite in the deeper parts of basalt source regions, then the possible influence of subducted crust on OIB petrogenesis requires understanding the partial melting behavior of bimineralic eclogite lithologies.

It should be noted that bimineralic garnet–pyroxene rocks fall on the so-called garnet–pyroxene thermal divide, which has a key influence on melting relations and liquid compositions produced from partial melting of synthetic and natural garnet pyroxenites at high

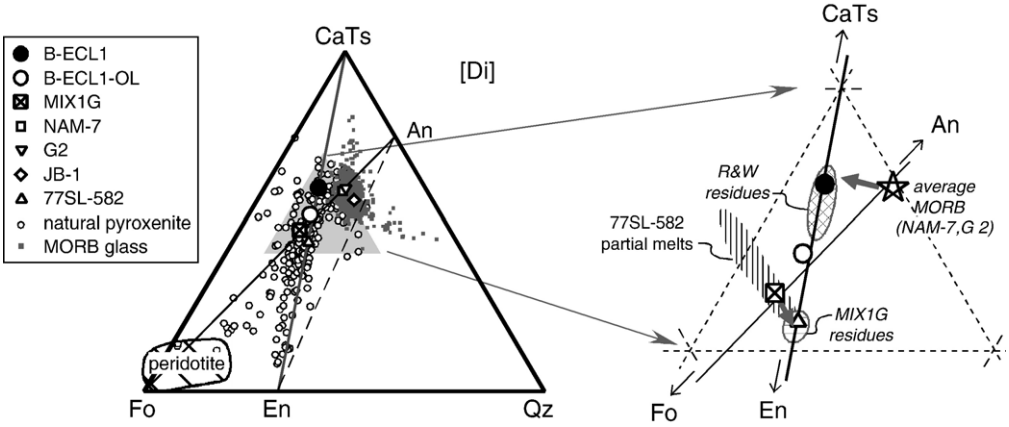

Fig. 1. Normative compositions of starting materials B-ECL1 and B-ECL1-OL in the pseudoternary system forsterite (Fo)–Ca-Tschermaks pyroxene (CaTs)–quartz (Qz) projected from diopside [Di] using the method of O'Hara [17]. Also plotted are silica-deficient pyroxenite MIX1G [4,5], bimineralic eclogite 77SL-582 [8], MORB-like pyroxenite NAM-7 [27] and G2 [6,7], alkali-rich basalt JB-1 [28], natural pyroxenites [1], MORB matrix glasses [33], and mantle peridotites [34]. Compositions of partial melts from 77SL-582 [8] and bimineralic residues of amphibolite dehydration melting (R&W residues [10]) and those of MIX1G [4,5] are indicated by hatched fields. Gray thick arrows indicate approximate paths of the pyroxenite residues to bimineralic compositions.

pressures [2,4,5,17]. This divide is defined by the enstatite (En)–Ca-tschermaks pyroxene (CaTs) join in the forsterite (Fo)–CaTs–quartz (Qz)–diopside (Di) normative diagram (Fig. 1) [17]. As classified by Hirschmann et al. [4], rocks composed chiefly of garnet and pyroxene with bulk compositions to the silica-enriched side of the divide are termed "silica-excess" pyroxenite and produce siliceous partial melts [3,6]; those to the silica-poor side of the join are "silica-deficient" pyroxenite and produce silica-poor partial melts [4,5]. Our previous experiments on an olivine-bearing garnet pyroxenite [4,5] demonstrated that certain silica-deficient pyroxenites can produce nepheline-normative liquids that closely resemble alkalic OIB. However, the melting behavior of bimineralic eclogite cannot be inferred directly from those of silica-excess and silica-deficient pyroxenites, because bimineralic eclogite by definition is neither silica-deficient nor silica-excess.

There are previous studies that did high-pressure melting experiments on bimineralic eclogite, but the melting behavior of bimineralic eclogite is not well documented because they had several shortcomings. The pioneering study was by O'Hara [18], but no phase compositions were reported. Ito and Kennedy [19] conducted more extensive experiments and analyses but employed Pt capsules and so their charges may have suffered iron loss. Adam et al. [20] investigated partial melting of bimineralic eclogite at 1.3–2 GPa, but these must have been (unintentionally) hydrous, as the product phases include amphibole. Keshav et al. [8] investigated partial melting of a nominally bimineralic Hawaiian pyroxenite, 77SL-582, at 2–2.5 GPa and found nepheline-normative partial melts with some similarities to alkalic OIB. However, reported compositions of 77SL-582 partial melts in equilibrium with garnet and pyroxene plot far from the thermal divide (Fig. 1). As elaborated in the Discussion below, this means that composition 77SL-582 must be silica-deficient, rather than bimineralic. Also composition 77SL-582 is quite different from expected residues of recycled oceanic crust (Fig. 1). Thus, the phase relations of bimineralic eclogite and the melt compositions produced by partial melting remain poorly known. In this study, we report results of partial melting experiments of a bimineralic eclogite at 3 and 5 GPa.

2. Experimental procedures

Starting material B-ECL1 was constructed from natural garnet and clinopyroxene powders and reagent SiO_2, TiO_2, Al_2O_3, and Na_2CO_3. Reagents were mixed under acetone and dried in an oven at 600 °C overnight, at 800 °C for 1 h, and at 1000 °C for 3 days to complete decarbonation. The decarbonated reagent mixture was then mixed with the garnet and clinopyroxene powders by grinding in agate under acetone for more than 1 h. The final mixture was dried at 1000 °C for 18 h in a $CO–CO_2$ gas stream near the quartz–fayalite–magnetite buffer and then ground in agate until it passed through a 15 μm screen. To determine how melting relations of bimineralic eclogite are modified by the presence of olivine, a second starting composition B-ECL1-OL was constructed from a mixture of B-ECL1 and 10 wt.% synthetic olivine of composition Fo_{60}. The olivine composition was selected to keep the bulk Mg# unchanged, so that the effect of olivine addition could be isolated from the influence of bulk Mg# variation [2].

Experiments were conducted at 3 and 5 GPa using a Kawai-type multi-anvil apparatus SPI-1000 at the Magma Factory, Tokyo Institute of Technology, using semi-sintered $MgO+Cr_2O_3$ octahedra with 18 mm edge lengths as pressure media, and WC cubes with 11 mm truncation edge lengths. The pressure was calibrated at 1200 °C using the following fixed points: quartz/coesite at 3.1 GPa [21], Fe_2SiO_4 olivine/spinel at 5.8 GPa [22], and coesite/stishovite at 9.2 GPa [23]. The furnace assembly consisted of a straight $LaCrO_3$ heater with Mo electrodes at the ends and Al_2O_3 and MgO inner pieces (Fig. 2). Sample powder was packed in a graphite crucible (inner size: 0.5 mm height 0.8 mm diameter) sealed in a Pt outer capsule. The assembled octahedra, furnace parts, and sample capsule were stored in a vacuum oven overnight at 220 °C before each experiment. Temperatures were measured using $W_{95}Re_5$–$W_{74}Re_{26}$ thermocouples. The thermal gradient in our assembly was investigated at 5 GPa and 1500 °C using an enstatite–diopside mixed powder and two-pyroxene

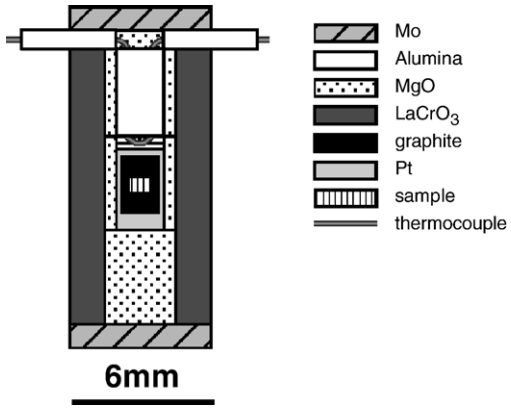

Fig. 2. Cross section of the furnace assembly used for the multi-anvil experiments.

Table 1
Compositions (wt.%) of starting materials of this study and pyroxenites used in past experimental studies

Name	SiO_2	TiO_2	Al_2O_3	Cr_2O_3	FeO*[a]	MnO	MgO	CaO	Na_2O	K_2O	Total	Mg#[b]
B-ECL1	46.0 (3)	1.72 (11)	15.7 (4)	0.04 (5)	10.6 (4)	0.21 (3)	10.1 (4)	12.5 (3)	2.47 (10)	0.04 (2)	99.31	62.9
B-ECL1-OL	46.7 (5)	1.51 (13)	13.6 (7)	0.03 (5)	12.4 (2)	0.19 (5)	11.6 (5)	11.4 (2)	2.24 (7)	0.04 (2)	99.69	62.4
MIX1G[c]	45.56	0.90	15.19	–	7.77	0.15	16.67	11.48	1.44	0.04	99.20	79.3
G2[d]	50.05	1.97	15.76	–	9.35	0.17	7.90	11.74	3.04	0.03	100.00	60.1
NAM-7[e]	49.70	1.71	15.70	–	9.37	0.18	8.43	11.73	2.76	0.23	99.81	61.6
JB-1[f]	53.25	1.37	14.83	0.05	8.36	0.17	7.89	9.48	2.85	1.46	99.71	62.7

[a] Total Fe as FeO.
[b] Mg# = molar Mg/(Mg + Fe) × 100.
[c] Hirschmann et al. [4], Kogiso et al. [5].
[d] Pertermann and Hirschmann [6,7].
[e] Yasuda et al. [27].
[f] Tsuruta and Takahashi [28].

thermometry of Nickel et al. [24]. The temperature difference across the sample position was found to be less than 30 °C.

Bulk compositions of starting materials are given in Table 1 and were determined by microprobe analyses of glasses quenched from 1500 °C and 1.5 GPa using a Boyd–England type piston cylinder apparatus at the Magma Factory and run procedures described in Kogiso et al. [15]. The starting compositions are plotted in the pseudoternary system Fo–CaTs–Qz projected from Di [17] in Fig. 1. In this projection, the B-ECL1 composition lies on the En–CaTs join, along which all stoichiometric garnets and pyroxenes plot, indicating that it is truly bimineralic. The composition of B-ECL1 is similar to bimineralic residues (garnet + clinopyroxene ± rutile) of dehydration melting of MORB-like amphibolites [10] (Fig. 1), suggesting that it is a plausible analog of altered oceanic crust that has undergone desilicification during subduction. The B-ECL1-OL composition is displaced slightly from the mixing line of B-ECL1 and olivine, probably owing to impurities in the Fo_{60} olivine powder, but nonetheless it plots to the olivine-enriched side of the En–CaTs join, indicating that it is silica-deficient.

Compositions of quenched phases in run charges were analyzed using a JEOL JXA8800 electron microprobe at Tokyo Institute of Technology. Analyses were done using a 15 kV, 12 nA beam and 10 to 20 s peak acquisition time. A fully focused beam (< 1 μm diameter)

Table 2
Run conditions and phase assemblages and proportions

Run no.	P (GPa)	T (°C)	Duration (h)	Phase[a]	Proportion[b]			$\sum r^2$
					melt	grt	cpx	
B-ECL1								
S1474	3.0	1450	24	gl, qch, grt, cpx	–	–	–	
S1479	3.0	1470	20	qch, grt, cpx	0.28 (4)	0.33 (2)	0.39 (3)	0.547
S1475	3.0	1500	20	gl, qch, grt, cpx	0.51 (3)	0.18 (2)	0.31 (2)	0.313
S1476	3.0	1550	10	gl, qch, grt, cpx				
S1477	3.0	1600	5	gl	–	–	–	
S1349	5.0	1500	24	grt, cpx	–	–	–	
S1359	5.0	1550	20	qch, grt, cpx	–	–	–	
S1342	5.0	1600	24	qch, grt, cpx	0.38 (5)	0.31 (4)	0.31 (3)	0.325
S1340	5.0	1650	24	gl, qch, grt, cpx	0.75 (7)	0.23 (3)	0.02 (5)	0.319
S1347	5.0	1675	5	gl, qch	–	–	–	
B-ECL1-OL								
S1425	5.0	1500	20	grt, cpx, ol	–	–	–	
S1424	5.0	1600	17	qch, grt, cpx	0.60 (4)	0.26 (2)	0.14 (3)	0.205
S1430	5.0	1650	3	qch, grt	0.86 (5)	0.14 (5)	–	1.26

[a] Abbreviations: gl = glass, qch = quench crystals, grt = garnet, cpx = clinopyroxene, ol = olivine.
[b] Numbers in parenthesis are two standard deviations and refer to the last digit.

Table 3
Compositions (wt.%) of melt and mineral phases[a]

Run no.	Phase[b]	n[c]	SiO_2	TiO_2	Al_2O_3	Cr_2O_3	FeO*	MnO	MgO	CaO	Na_2O	K_2O	Total	Mg#	K_D[d]
B-ECL1															
S1479	melt	7	46.4 (6)	3.9 (6)	13.4 (4)	0.03 (5)	13.2 (9)	0.19 (3)	7.3 (5)	11.6 (10)	3.7 (4)	0.03 (10)	99.74	49.6	
(3GPa, 1470 °C)	grt	11	41.1 (5)	1.0 (2)	22.1 (5)	0.04 (7)	14.1 (4)	0.36 (6)	12.5 (5)	9.6 (3)	0.1 (1)	0.00 (1)	100.89	61.2	0.62
	cpx	9	51.3 (5)	1.0 (2)	12.6 (6)	0.03 (5)	6.4 (3)	0.13 (4)	10.2 (4)	15.2 (7)	3.7 (3)	0.00 (1)	100.52	73.9	0.35
S1475	melt	32	46.3 (7)	2.6 (1)	14.9 (3)	0.01 (3)	12.5 (4)	0.21 (5)	8.0 (2)	11.4 (3)	3.2 (2)	0.06 (3)	99.27	53.5	–
(3GPa, 1500 °C)	grt	13	40.7 (9)	1.0 (3)	23.0 (4)	0.04 (6)	12.6 (8)	0.37 (6)	13.7 (7)	9.1 (5)	0.1 (1)	0.02 (2)	100.61	66.0	0.59
	cpx	15	49.5 (7)	1.0 (2)	13.6 (5)	0.03 (4)	6.2 (4)	0.14 (5)	10.8 (3)	15.8 (5)	3.0 (2)	0.02(3)	100.02	75.7	0.37
S1342	melt	9	45.7 (9)	3.6 (4)	12.8 (2)	0.02 (5)	14.0 (3)	0.24 (9)	7.4 (3)	12.6 (7)	3.0 (1)	0.06 (5)	99.46	48.6	–
(5GPa, 1600 °C)	grt	13	41.2 (6)	0.9 (2)	22.8 (3)	0.05 (7)	12.2 (5)	0.35 (6)	13.2 (9)	10.5 (6)	0.2 (0)	0.02 (4)	101.39	65.9	0.49
	cpx	15	51.9 (6)	0.7 (2)	12.8 (9)	0.04 (6)	5.7 (4)	0.11 (5)	10.4 (5)	15.1 (5)	3.6 (2)	0.02 (3)	100.47	76.5	0.29
S1340	melt	16	47.3 (5)	2.1 (3)	13.9 (3)	0.01 (4)	11.1 (4)	0.20 (3)	8.7 (3)	13.5 (5)	2.9 (1)	0.04 (3)	99.81	58.3	–
(5GPa, 1650 °C)	grt	13	41.7 (6)	0.7 (2)	22.7 (5)	0.07 (5)	10.0 (10)	0.32 (6)	14.0 (12)	11.0 (6)	0.2 (1)	0.02 (2)	100.65	71.3	0.56
	cpx	11	51.5 (8)	0.5 (1)	12.8 (12)	0.04 (4)	4.7 (5)	0.13 (6)	10.8 (6)	16.2 (4)	3.5 (1)	0.02 (3)	100.24	80.4	0.34
B-ECL1-OL															
S1424	melt	11	47.4 (10)	2.2 (10)	10.9 (8)	0.01 (4)	13.9 (15)	0.17 (7)	9.4 (7)	12.3 (8)	2.8 (3)	0.04 (3)	99.05	54.7	–
(5GPa, 1600 °C)	grt	20	41.6 (6)	0.7 (2)	22.5 (8)	0.05 (5)	12.2 (8)	0.27 (7)	14.9 (8)	8.4 (5)	0.2 (1)	0.02 (2)	100.74	68.5	0.55
	cpx	15	53.0 (8)	0.4 (1)	10.1 (4)	0.03 (4)	6.3 (4)	0.11 (6)	12.4 (5)	14.7 (4)	3.3 (3)	0.02 (2)	100.31	77.8	0.34
S1430	melt	5	47.9 (7)	1.3 (4)	12.2 (2)	0.02 (3)	12.1 (7)	0.17 (7)	11.1 (7)	12.5 (5)	2.5 (2)	0.04 (2)	99.78	61.9	–
(5GPa, 1650 °C)	grt	16	41.9 (7)	0.5 (1)	23.3 (5)	0.05 (5)	9.3 (5)	0.19 (6)	16.5 (6)	9.1 (5)	0.1 (1)	0.02 (2)	100.90	76.0	0.51

[a]Numbers in parenthesis are two standard deviations and refer to the last digit(s).
[b]Phase abbreviations as in Table 2.
[c]Number of analysis.
[d]Fe–Mg exchange coefficient (in mol) between mineral and melt: $(Fe/Mg)_{mineral}/(Fe/Mg)_{melt}$.

was used to analyze mineral phases, and a defocused beam (5–20 μm diameter) was used to analyze quenched melt phases. Analytical precision for major oxides is better than 2% relative [5]. Phase proportions were calculated by mass balance between the composition of coexisting phases and the bulk composition using a linear least squares method. Residual sums of squares range from 0.2 to 1.2 (Table 2).

3. Results

3.1. Phase relations

Experimental conditions and phase assemblages are listed in Table 2 and melt and mineral compositions in Table 3. Crystal sizes range from 5 to 10 μm in sub-solidus runs to ~50 μm in near-liquidus runs. Clinopyroxene crystals show no detectable compositional zoning, but small (<5 μm) relict cores remain in some garnet grains in all runs. These cores have negligible influence on phase equilibria and mass balance, as they are restricted to a small number of relatively large (>10 μm) grains, even in low-temperature runs (e.g., S1474). Quenched melt portions consist of glass and/or mattes of fine-grained quench crystals. Oxide totals of melt compositions are above 99 wt.%, indicating that dissolved volatile concentrations are small. Fe–Mg exchange coefficients, K_D (=$(Fe/Mg)_{mineral}/(Fe/Mg)_{melt}$), are 0.55±0.07 and 0.33±0.04 for garnet and clinopyroxene, respectively, which are broadly consistent with previous pyroxenite partial melting experiments at >2 GPa [4,5].

The sub-solidus mineral assemblages of B-ECL1 and B-ECL1-OL are garnet+clinopyroxene and garnet+clinopyroxene+olivine, respectively (Table 2). Above the solidi, garnet and clinopyroxene coexist with melt below 1500 °C at 3 GPa in B-ECL1 and below 1600 °C at 5 GPa in both compositions. At 3 GPa, the residual garnet/clinopyroxene ratio in B-ECL1 decreases with increasing temperature (Table 2), suggesting that clinopyroxene is the liquidus phase. At 5 GPa, clinopyroxene is nearly consumed in B-ECL1 and absent in B-ECL1-OL (Table 2) at 1650 °C, suggesting that garnet is the liquidus phase at this pressure in both compositions. Temperature–melt fraction curves for B-ECL1 and B-ECL1-OL are shown in Fig. 3. The solidus of B-ECL1 is located below 1450 °C at 3 GPa and between 1500 and 1550 °C at 5 GPa, and its liquidus is between 1550 and 1600 °C at 3 GPa and between 1650 and 1675 °C at 5 GPa. The solidus and liquidus of B-ECL1-OL were not determined directly, but comparison of temperature–melt fraction curves suggests that they are just slightly cooler than those of B-ECL1 (Fig. 3b).

3.2. Melt and mineral compositions

Partial melt compositions (Table 3) are plotted in the Fo–CaTs–Qz normative projection in Fig. 4 and against MgO contents in Fig. 5. Partial melts from B-ECL1 at 3 and 5 GPa lie along the En–CaTs join (Fig. 4), which is consistent with this join acting as a thermal crest. Partial melts from B-ECL1-OL plot near the join, but are displaced to the silica-deficient side, as expected for a silica-deficient bulk composition [4] (Fig. 1). Partial melts of both B-ECL1 and B-ECL1-OL have less silica than compositions defining the Fo–An join (Fig. 4), meaning that they are nepheline-normative, and have compositions akin to primitive (7.4–11.1 wt.% MgO)

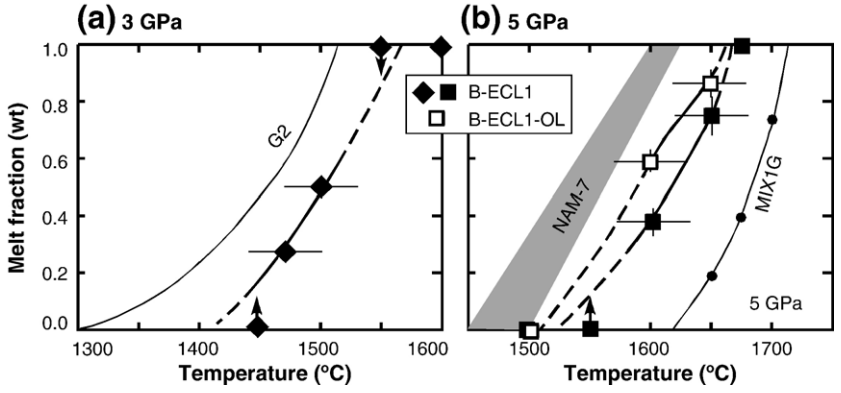

Fig. 3. Temperature–weight fraction curves of partial melts produced from B-ECL1 and B-ECL1-OL (this study), MORB-like pyroxenite G2 [6,7], and MIX1G [5] determined by mass balance calculations. Error bars are ±30 °C for temperature (see text) and two standard deviations in mass balance calculation (Table 2). Errors less than the size of symbols are not shown. Symbols with arrow indicate the upper/lower limit of melt fraction. Dark field is estimated position of the melt fraction trend for the MORB-like pyroxenite NAM-7 at 5 GPa [27].

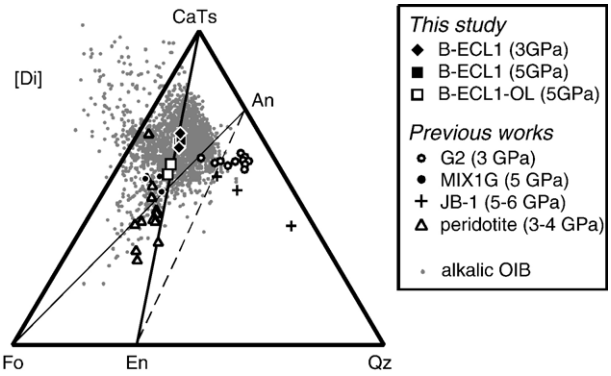

Fig. 4. Compositions of partial melts of B-ECL1 and B-ECL1-OL in the pseudoternary Fo–CaTs–Qz diagram projected from Di. Also plotted are experimental partial melts of MIX1G produced at 5 GPa [5], MORB-like pyroxenite G2 at 3 GPa [6], alkali-rich basalt JB-1 at 5 to 6 GPa [28], peridotite at 3 to 5 GPa [35–37], and alkalic OIB [5].

alkalic OIB (Fig. 5). With increasing pressure, the partial melts produced from B-ECL1 become richer in CaO and poor in Al_2O_3 and Na_2O at a given MgO, reflecting higher garnet/clinopyroxene ratio in the residue (Table 2) and more compatible behavior of Na_2O in clinopyroxene (Table 3) at higher pressure, as demonstrated previously (e.g., [2,5]). With increasing temperature, CaO contents decrease at 3 GPa but

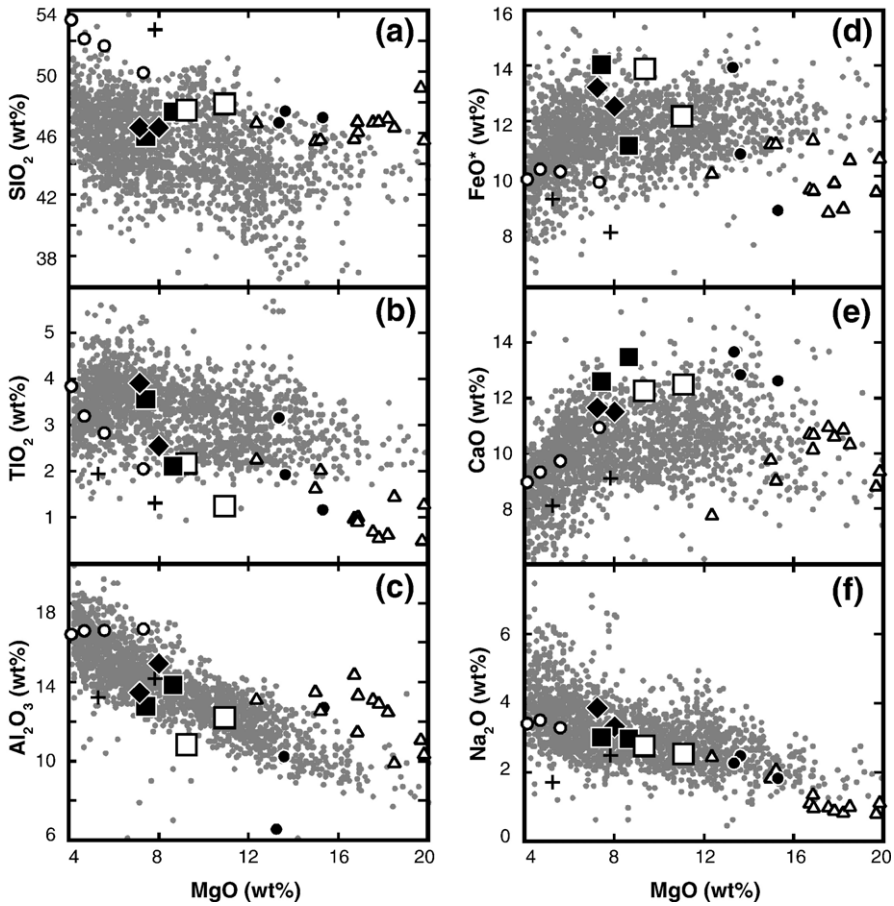

Fig. 5. Compositions of partial melts of B-ECL1 and B-ECL1-OL and those from previous studies plotted against MgO contents. Symbols and data sources are as in Fig. 4.

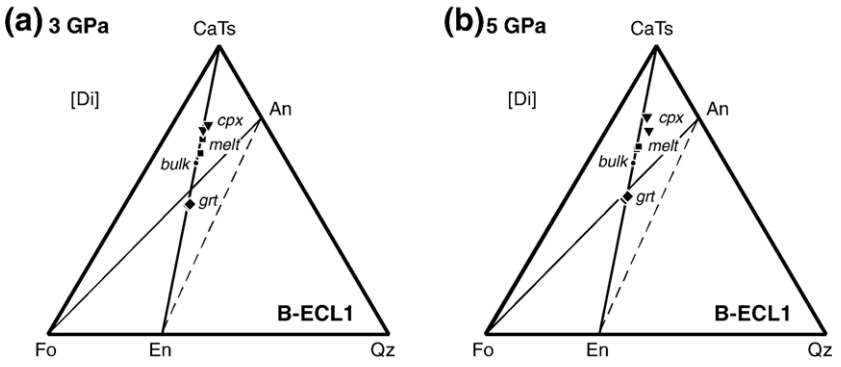

Fig. 6. Melting relations of B-ECL1 with melt and residual minerals in the Fo–CaTs–Qz diagram projected from Di. The melt composition is intermediate between that of garnet (grt) and clinopyroxene (cpx), which suggests that the melting relation is eutectic-like both at 3 and 5 GPa.

increase at 5 GPa (Table 3 and Fig. 5e), because clinopyroxene is consumed more rapidly at 5 GPa (Table 2). Al_2O_3 and MgO contents increase, and TiO_2, FeO*, and Na_2O contents decrease with increasing temperature both at 3 and 5 GPa (Fig. 5). Compared to those from B-ECL1, the partial melts of B-ECL1-OL are slightly enriched in MgO and depleted in Al_2O_3 TiO_2, Na_2O, and CaO (Fig. 5), reflecting differences in bulk compositions.

Mineral compositions are plotted in the Fo–CaTs–Qz normative projection (Fig. 6). Pyroxenes are Na_2O- and Al_2O_3-rich (3.0–3.7 wt.% and 10.1–13.6 wt.%, respectively, Table 3), reflecting a significant jadeite component (~21–26 mol%). Their stoichiometries indicate small (0.2–2.2%) apparent vacancy concentrations in the M2 site, possibly reflecting a modest component of Ca-eskolaite [25]. Although such pyroxenes have slight silica excesses relative to the stoichiometric garnet–pyroxene join on the Fo–CaTs–Qz projection (Fig. 6), their displacement is small and probably does not diminish appreciably the influence of the thermal crest along the join. Garnet compositions are Ca-rich, with 22–28% grossular component (Table 3).

4. Discussion

4.1. Effect of composition and mineralogy on pyroxenite and eclogite solidi

It is commonly assumed that bimineralic residues resulting from melt extraction from more complex pyroxenites are refractory (e.g., [26]). This reasoning derives from observations in the simple CaO–MgO–Al_2O_3–SiO_2 system, for which bimineralic eclogite has a higher solidus temperature than silica-excess and silica-deficient pyroxenites (e.g., [17]). However, Kogiso et al. [2] showed that solidus temperatures of natural pyroxenites and eclogites depend chiefly on bulk alkali content and/or Mg# and are little influenced by their position relative to the thermal divide. This may be because the bulk compositions reviewed by Kogiso et al. [2] varied considerably in alkalis and Mg#. In contrast, B-ECL1 and B-ECL1-OL have very similar Mg# and bulk alkali contents but different positions relative to the thermal crest (Fig. 1), so their melting behaviors isolate the effect of the divide in natural systems. The slightly higher solidus for B-ECL1 compared to B-ECL1-OL (Fig. 3b) indicates that bimineralic eclogite is more refractory than a more mineralogically complex pyroxenite with similar alkali content and Mg#. However, the solidus temperature is less affected by exhaustion of minerals and is chiefly influenced by bulk alkali contents.

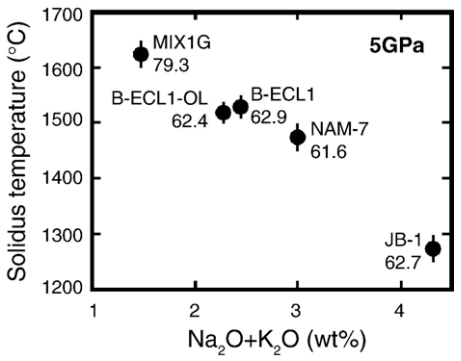

Fig. 7. Solidus temperatures of various pyroxenite compositions experimentally determined at 5 GPa (B-ECL1 and B-ECL1-OL: this study, MIX1G: [5], NAM-7: [27], JB-1: [28]) correlate with bulk Na_2O+K_2O content. Numbers indicate Mg#. The similar solidi of B-ECL1 and B-ECL1-OL indicate that the bulk alkali content influences solidi more than the mineralogic complexity of the residue.

The importance of bulk alkali content to solidus temperatures of pyroxenites is well illustrated by comparison of the 5 GPa solidi of B-ECL1 and B-ECL1-OL to those of Mix1G [5], NAM7 [27] and JB-1 [28] (Fig. 7). Mix1G has sub-solidus olivine and has a higher Mg# and lower total alkalis than B-ECL1±OL. NAM-7 and JB-1 have sub-solidus coesite and have a similar Mg# and higher total alkalis than B-ECL1±OL. JB-1 also has sub-solidus alkali feldspar. As shown in Fig. 7, observed solidus temperatures for these diverse mineralogies diminish linearly with total alkalis irrespective of their position relative to the thermal divide (Fig. 1). The large range of solidi among B-ECL1, B-ECL1-OL, NAM-7, and JB-1 is observed even though these lithologies have quite similar Mg#s (61.6 to 62.9: Table 1 and Fig. 7), suggesting that alkali concentrations rather than Mg#s are the chief compositional factor influencing solidi at high pressure. The bimineralic character of a pyroxenite or eclogite is a minor influence on the solidus.

Given the significant influence of alkalis on the solidi of eclogite and pyroxenite compositions, melt removal increases the melting temperature of pyroxenites owing to diminished alkalis in the residual minerals. However, large increases in solidus temperature may require considerable melting, as alkalis are compatible or mildly incompatible in pyroxenes at high pressure. For example, values of $D_{Na}^{cpx/melt}$ observed in partial melting experiments at 3–5 GPa range from 0.6 to 1.2 (this study; [3,5,6]).

4.2. Melting relations and production of nepheline-normative liquids

An important observation regarding partial melts of bimineralic eclogite B-ECL1 is that they are nepheline-normative (Fig. 4). Partial melts from B-ECL1 at 3 and 5 GPa must lie on the garnet–pyroxene thermal divide in the Fo–CaTs–Qz normative projection (Figs. 1 and 4) because the B-ECL1 bulk composition as well as the residual phases all lie on the divide (Fig. 1). However, the thermal divide spans both nepheline-normative and hypersthene-normative compositions, so in theory partial melts from bimineralic eclogite could be alkalic or tholeiitic. The key is that garnet+clinopyroxene partially melt at a eutectic-like minimum along the thermal divide (Fig. 6). As the "eutectic" point plots within the nepheline-normative field, any bimineralic eclogites that consist of garnet and clinopyroxene with compositions similar to those of B-ECL1 can produce nepheline-normative liquids at this pressure range. Thus, partial melts of bimineralic eclogite will be alkalic over a wide range of bulk compositions and pressures because bimineralic residua resulting from fluid or melt extraction from many pyroxenites, including typical subducted crust compositions, are expected to be nepheline-normative (Fig. 1). It is also possible that bimineralic residues with compositions that are not nepheline-normative, such as those derived from garnet pyroxenite MIX1G (Fig. 1), could also produce nepheline-normative eutectic-like melts. This suggests that residues of recycled subducted crust can produce alkali basaltic magmas within the pressure interval (~3–5 GPa) likely in OIB source regions beneath thick lithosphere.

Partial melts of nominally bimineralic pyroxenite 77SL-582 reported by Keshav et al. [8] coexisting with only garnet and pyroxene have much less silica than compositions that define the En–CaTs thermal divide (Fig. 1). This can only be explained if the rock used by Keshav et al. [8] falls to the silica-deficient side of the divide, meaning that the bulk composition that they report must be in error. This conclusion is also suggested by the high K_2O contents (0.2–1.3 wt.% K_2O) in their reported glasses, which, when combined with reported melt fractions, suggest bulk K_2O between 0.2 and 0.5 wt.% (*cf.* 0.09 wt.% reported bulk K_2O). Such large K_2O contents are unlikely for a rock consisting of garnet and pyroxene only, and imply that the experiments of Keshav et al. [8] were influenced by an unidentified potassic phase.

4.3. Genesis of alkalic OIB

The B-ECL1 and B-ECL1-OL partial melts have major-element characteristics similar to many alkalic OIB, including low Al_2O_3 and SiO_2 and high FeO* and CaO contents (Fig. 5), as well as similar TiO_2 and Na_2O contents. Owing to eutectic-like melting behavior (Fig. 6), near-solidus partial melts should not be significantly different from those at higher melt fractions, although composition–melt fraction trends suggest that near-solidus partial melts will be lower in Al_2O_3 and higher in FeO, TiO_2 and Na_2O than the intermediate melt fractions documented here and alkalic OIB (Tables 2 and 3, Fig. 5). As noted by Kogiso et al. [5], the low Al_2O_3 and high FeO* of alkalic OIB are distinct from experimentally produced partial melts of peridotite, carbonated peridotite, or peridotite+basalt mixtures (Fig. 5), suggesting that some sources other than peridotite are necessary to account for the low Al_2O_3 and high FeO* of alkalic OIB. Such a low-Al_2O_3 and high-FeO component can be produced by partial melting of B-ECL1 and B-ECL1-OL, because Al_2O_3

and FeO* contents of B-ECL1 and B-ECL1-OL melts are comparable to (or potentially much lower/higher than) those of alkalic OIB. On the other hand, the MgO contents of B-ECL1 and B-ECL1-OL partial melts do not exceed ~11 wt.% MgO, which is lower than that found in the most primitive alkalic OIB (Fig. 5). Thus, the partial melts are not sufficiently magnesian to be parental to most primitive OIB lavas, yet they may contribute a low-Al_2O_3 and high-FeO component to alkalic OIB, provided that such primitive lavas also derive in part from partial melting of some kind of peridotite.

Ideally, experimental liquids (or blends of such liquids) that are potentially parental to OIB should be compared to plausible primary OIB compositions. However, many OIB have been affected by crystal fractionation and/or accumulation involving olivine and/or clinopyroxene. Correcting primitive OIB lavas for these effects requires detailed investigations on natural rock samples, which are beyond the scope of this paper. However, OIB primary liquids must lie within observed OIB compositional trends. Because the low-Al_2O_3 and high-FeO* trends observed in alkali OIB are not matched by existing experiments on peridotite partial melt trends, an additional source, including possibly bimineralic eclogite partial melts, must contribute to their petrogenesis (Fig. 5).

Keshav et al. [8] questioned the possible role of mafic lithologies in the genesis of alkalic OIB because compositional variation among alkalic OIB suites do not originate from variable degrees of partial melting of a garnet pyroxenite 77SL-582. We consider this reasoning to be puzzling — the widely observed isotopic variations within and among OIB suites argue strongly against an origin by variable degrees of partial melting of a single source. The chief argument of Keshav et al. [8] is that partial melts of garnet pyroxenite form trends on major element diagrams that intersect those of alkalic OIB at high angle. However, this argument has little to do with whether partial melts of pyroxenite may contribute a component of melt to alkalic OIB.

4.4. Melting of recycled oceanic crust in OIB source regions

As described above, the composition of B-ECL1 is analogous to desilicified subducted oceanic crust (Fig. 1), and its high-pressure partial melts are alkalic and may be plausible sources of low-Al_2O_3, high-FeO* components in OIB (Figs. 4 and 5). If bimineralic eclogite of recycled-crust origin is present as minor domains in upwelling peridotite, its partial melts may be blended with high MgO liquids derived from partial melts of surrounding peridotite. Because the solidus temperature of B-ECL1 is lower than that of typical mantle peridotite (1600–1650 °C at 5 GPa: [29,30]), bimineralic eclogite in the upwelling mantle begins to melt deeper than surrounding peridotite. Partial melts from bimineralic eclogite domains will be transported to shallower regions where peridotite itself partially melts, and then be mixed with peridotite-derived high-MgO liquids. Mixing with peridotite-derived melts will increase MgO contents with no significant change in Al_2O_3 contents (Fig. 5c), resulting in production of low-Al_2O_3 liquids having high MgO contents.

There remain several problems to be clarified for understanding how primitive OIB-like magmas can be produced by processes involving partial melting of bimineralic eclogite and peridotite. First, prior to extraction from their source, partial melts within bimineralic eclogite domains may change their compositions by diffusive interaction with surrounding peridotite. However, this process will not significantly influence major element compositions of bimineralic eclogite partial melts if pyroxenite domains are larger than several meters thick [13]. Second, once they are extracted from their pyroxenitic source, partial melts may react with peridotite. This process has been investigated experimentally for the case where the partial melts are silicic, in which case the melts freeze and metasomatize the peridotite [3]. In contrast, invading partial melts of bimineralic eclogite could promote partial melting of surrounding peridotite, as nepheline-normative melts may dissolve peridotitic pyroxene [31,32], but the quantitative effect on melt compositions is not well constrained experimentally. The importance of reaction between partial melts and surrounding peridotite clearly depends on the trade off between the length scale of pyroxenitic domains and the distance between the domains and available fast paths (dunite channels or dikes) leading to melt ascent.

A different scenario, considered by Yaxley and Green [3], Lundstrom [31], and Sobolev et al. [26], emphasizes the importance of reaction between partial melts of pyroxenite and surrounding peridotite. In this case, initial partial melts of pyroxenite infiltrate and react with peridotite, forming a reaction skarn and leaving behind a bimineralic residue. The mineralogy of the reaction skarn depends on the composition of the infiltrating melt, the pressure, and the local proportions of melt added. The resulting suite of diverse lithologies may be geochemically complex and are potentially rich in fertile components and

incompatible elements. If the hybridized lithologies are peridotitic, they can produce MgO-rich alkalic partial melts [3], but it remains unclear whether such liquids have specific compositions similar to alkalic OIB. Sobolev et al. [26] posit that the hybridized rocks may become more fertile than the residual eclogite, because they assume that bimineralic rocks become highly refractory. If this were so, it would help account for trace element fractionations in OIB source regions as the limited melting of the original vein material would hold back key elements (such as heavy rare earth elements). However, our results cast doubt on this assumption. So long as the pyroxenes in residual bimineralic eclogite retain significant alkalis (and have low Mg#) compared to surrounding hybridized peridotite, we expect that residual vein material will continue to be quite fertile (Fig. 7). For example, hybridized layers formed in coesite eclogite/garnet peridotite reaction experiments by Yaxley and Green [3] at 3.5 GPa have higher Mg#s, lower total alkalis, and lower melt fractions than neighboring residual bimineralic eclogite at all temperatures investigated.

5. Conclusions

Bimineralic eclogite is a variety of pyroxenite that is the residue of melt or fluid extraction from a wide variety of more complex pyroxenites, including eclogite derived from subducted mafic oceanic crust. Partial melting experiments at 3 and 5 GPa on a bimineralic eclogite with and without small amounts of olivine demonstrate that bimineralic eclogite produces nepheline-normative basaltic liquids with low Al_2O_3 and high FeO* contents, which are similar to alkalic OIB lavas. Although these partial melts have much lower MgO contents than primitive alkalic OIB, partial melting of bimineralic recycled crust can produce a liquid component with low Al_2O_3 and high FeO*, which are necessary for the genesis of alkalic OIB.

Acknowledgments

We thank Eiichi Takahashi for his great support for the high-pressure experiments at the Magma Factory. We also thank Toshihiro Suzuki and Yu Nishihara for providing us with synthetic pyroxenes and olivine, V. Rama Murthy for natural garnet and clinopyroxene, and Shun Karato and Daisuke Yamazaki for help with their gas-mixture furnace. We acknowledge constructive reviews by Sébastien Pilet and an anonymous reviewer. This work was supported by a MEXT grant 15740318 to TK and NSF grant OCE9876255 to MMH.

References

[1] M.M. Hirschmann, E.M. Stolper, A possible role for garnet pyroxenite in the origin of the “garnet signature” in MORB, Contrib. Mineral. Petrol. 124 (1996) 185–208.
[2] T. Kogiso, M.M. Hirschmann, M. Pertermann, High pressure partial melting of mafic lithologies in the mantle, J. Petrol. 45 (2004) 2407–2422.
[3] G.M. Yaxley, D.H. Green, Reactions between eclogite and peridotite: mantle refertilisation by subduction of oceanic crust, Schweiz. Mineral. Petrogr. Mitt. 78 (1998) 243–255.
[4] M.M. Hirschmann, T. Kogiso, M.B. Baker, E.M. Stolper, Alkalic magmas generated by partial melting of garnet pyroxenite, Geology 31 (2003) 481–484.
[5] T. Kogiso, M.M. Hirschmann, D.J. Frost, High-pressure partial melting of garnet pyroxenite: possible mafic lithologies in the source of ocean island basalts, Earth Planet. Sci. Lett. 216 (2003) 603–617.
[6] M. Pertermann, M.M. Hirschmann, Anhydrous partial melting experiments on MORB-like eclogite: phase relations, phase compositions and mineral–melt partitioning of major elements at 2–3 GPa, J. Petrol. 44 (2003) 2173–2201.
[7] M. Pertermann, M.M. Hirschmann, Partial melting experiments on a MORB-like pyroxenite between 2 and 3 GPa: constraints on the presence of pyroxenites in basalt source regions from solidus location and melting rate, J. Geophys. Res. 108 (2003) 2125, doi:10.1029/2000JB000118.
[8] S. Keshav, G.H. Gudfinnsson, G. Sen, Y. Fei, High-pressure melting experiments on garnet clinopyroxenite and the alkalic to tholeiitic transition in ocean-island basalts, Earth Planet. Sci. Lett. 223 (2004) 365–379.
[9] C.E. Manning, The solubility of quartz in H_2O in the lower crust and upper mantle, Geochim. Cosmochim. Acta 58 (1994) 4831–4839.
[10] R.P. Rapp, E.B. Watson, Dehydration melting of metabasalt at 8–32 kbar; implications for continental growth and crust–mantle recycling, J. Petrol. 36 (1995) 891–931.
[11] R. Kessel, M.W. Schmidt, P. Ulmer, T. Pettke, Trace element signature of subduction-zone fluids, melts and supercritical liquids at 120–180 km depth, Nature 437 (2005) 724–747.
[12] A. Tabit, J. Kornprobst, A.B. Woodland, The garnet peridotites of the Beni Bousera Massif (Morocco): tectonic mixing and iron–magnesium interdiffusion, Comptes Rendus— Academie des Sciences, Serie II: Sciences de la Terre et des Planetes, vol. 325, 1997, pp. 665–670.
[13] T. Kogiso, M.M. Hirschmann, P.W. Reiners, Length scales of mantle heterogeneities and their relationship to ocean island basalt geochemistry, Geochim. Cosmochim. Acta 68 (2004) 345–360.
[14] T. Kogiso, Y. Tatsumi, G. Shimoda, H.G. Barsczus, High μ (HIMU) ocean island basalts in southern Polynesia: new evidence for whole-mantle scale recycling of subducted oceanic crust, J. Geophys. Res. 102 (1997) 8085–8103.
[15] T. Kogiso, K. Hirose, E. Takahashi, Melting experiments on homogeneous mixtures of peridotite and basalt: application to the genesis of ocean island basalts, Earth Planet. Sci. Lett. 162 (1998) 45–61.
[16] Y. Niu, M.J. O’Hara, Origin of ocean island basalts: a new perspective from petrology, geochemistry, and mineral physics considerations, J. Geophys. Res. 108 (2003), doi:10.1029/2002JB002048.

[17] M.J. O'Hara, The bearing of phase equilibria studies in synthetic and natural systems on the origin and evolution of basic and ultrabasic rocks, Earth-Sci. Rev. 4 (1968) 69–133.
[18] M.J. O'Hara, Melting of bimineralic eclogite at 30 kilobars, Carnegie Insititution of Washington Yearbook, vol. 62, 1963, pp. 76–77.
[19] K. Ito, G.C. Kennedy, The composition of liquids formed by partial melting of eclogites at high temperatures and pressures, J. Geol. 82 (1974) 383–392.
[20] J. Adam, T.H. Green, R.A. Day, An experimental study of two garnet pyroxenite xenoliths from the Bullenmerri and Gnotuk Maars of western Victoria, Australia, Contrib. Mineral. Petrol. 111 (1992) 505–514.
[21] S.R. Bohlen, A.L. Boettcher, The quartz–coesite transformation: a precise determination and the effects of other components, J. Geophys. Res. 87 (1982) 7073–7078.
[22] T. Yagi, M. Akaogi, O. Shimomura, T. Suzuki, S. Akimoto, In situ observation of the olivine-spinel phase transformation in Fe_2SiO_4 using synchrotron radiation, J. Geophys. Res. 92 (1987) 6207–6213.
[23] J. Zhang, B. Li, W. Utsumi, R.C. Liebermann, In situ X-ray observations of the coesite–stishovite transition: reversed phase boundary and kinetics, Phys. Chem. Miner. 23 (1996) 1–10.
[24] K.G. Nickel, G.P. Brey, L. Kogarko, Orthopyroxene–clinopyroxene equilibria in the system $CaO–MgO–Al_2O_3–SiO_2$ (CMAS): new experimental results and implications for two-pyroxene thermometry, Contrib. Mineral. Petrol. 91 (1985) 44–53.
[25] T.C. McCormick, Crystal-chemical aspects of nonstoichiometric pyroxenes, Am. Mineral. 71 (1986) 1434–1440.
[26] A.V. Sobolev, A.W. Hofmann, S.V. Sobolev, I.K. Nikogosian, An olivine-free mantle source of Hawaiian shield basalts, Nature 434 (2005) 590–597.
[27] A. Yasuda, T. Fujii, K. Kurita, Melting phase relations of an anhydrous mid-ocean ridge basalt from 3 to 20 GPa: implications for the behavior of subducted oceanic crust in the mantle, J. Geophys. Res. 99 (1994) 9401–9414.
[28] K. Tsuruta, E. Takahashi, Melting study of an alkali basalt JB-1 up to 12.5 GPa: behavior of potassium in the deep mantle, Phys. Earth Planet. Inter. 107 (1998) 119–130.
[29] M.M. Hirschmann, The mantle solidus: experimental constraints and the effect of peridotite composition, Geochem. Geophys. Geosyst. 1 (2000) (2000GC000070).
[30] C.E. Lesher, J. Pickering-Witter, G. Baxter, M.J. Walter, Melting of garnet peridotite: effects of capsules and thermocouples, and implications for the high-pressure mantle solidus, Am. Mineral. 88 (2003) 1181–1189.
[31] C.C. Lundstrom, Rapid diffusive infiltration of sodium into partially molten peridotite, Nature 403 (2000) 527–530.
[32] M. Lo Cascio, Y. Liang, P.C. Hess, Grain-scale processes during isothermal-isobaric melting of lherzolite, Geophys. Res. Lett. 31 (2004), doi:10.1029/2004GRL020602.
[33] W.G. Melson, T. O'Hearn, P. Kimberly, Volcanic glasses from sea-floor spreading centers and other deep sea tectonic settings: major and minor element compositions in the Smithsonian WWW Data Set (abstract), EOS, Trans. - Am. Geophys. Union 80 (1999) F1177.
[34] C. Herzberg, M. Feigenson, C. Skuba, E. Ohtani, Majorite fractionation recorded in the geochemistry of peridotites from South Africa, Nature 332 (1988) 823–826.
[35] K. Hirose, I. Kushiro, Partial melting of dry peridotites at high pressures: determination of compositions of melts segregated from peridotite using aggregates of diamond, Earth Planet. Sci. Lett. 114 (1993) 477–489.
[36] I. Kushiro, Partial melting of a fertile mantle peridotite at high pressures: an experimental study using aggregates of diamond, in: A. Basu, S. Hart (Eds.), Earth Processes: Reading the Isotopic Code, Geophysical Monograph, vol. 95. American Geophysical Union, Washington D.C., 1996, pp. 109–122.
[37] M.J. Walter, Melting of garnet peridotite and the origin of komatiite and depleted lithosphere, J. Petrol. 39 (1998) 29–60.